2

Constitutive modelling for composite forming

R AKKERMAN and E A D LAMERS, University of Twente, The Netherlands

2.1 Introduction

Fibre reorientation occurs when forming a reinforced structure, such as a fabric onto a doubly curved surface. This leads to a change in the angle between warp and fill yarns. The composite properties change inhomogeneously, corresponding to the varying angle between warp and fill yarns. Many composite properties are determined by the angle between the warp and fill yarns, such as the mechanical properties, the coefficients of thermal expansion, the local fibre volume fractions, the local thickness and the permeability. The extent of the fibre reorientation is affected by the product shape and the forming process. The forming process may cause tensile stresses in the fabric yarns, causing subsequent product distortions. Also, wrinkling risks are present due to the incapability of the fabric to deform beyond a maximum shear deformation. The local change in composite properties must be taken into account in order to predict the properties of a product. Drape modelling can predict the process induced fibre orientations and stresses, which can speed up the product development process compared with trial-and-error development. The constitutive model for these biaxially reinforced composite materials is the primary element of these process simulations.

2.2 Review on constitutive modelling for composite forming

Both dry and pre-impregnated fabrics can be draped over a mould during the composite forming process. When forming a dry fabric over the mould, the result is a preform. This preform can be impregnated subsequently with a polymer, for instance in one of the Liquid Composite Moulding (LCM) processes.

When draping pre-impregnated composites, the fabric is embedded in the matrix material. In the case of thermoplastics, several plies can be stacked into a pre-consolidated laminate preform. This preform is heated above the glass

transition or melting temperature of the polymer matrix, formed on the tool and subsequently cooled or cured until the product is form stable.

Various drape models for dry and pre-impregnated fabrics have been proposed in the past. Lim and Ramakrishna published a review in 2002 on the forming of composite sheet forming. Two approaches are distinguished in their review: the mapping approach and the mechanics approach. The use of mapping approaches is discussed in Chapter 12, whilst the mechanical modelling of forming is described in Chapter 3. Here, we will concentrate on the underlying constitutive models, using a different classification: the discrete approach and the continuum approach. This classification is based on the representation of the material by the models. Draping multi-layered composites gives rise to additional complexity which will be discussed subsequently.

2.2.1 Discrete models

Three schemes are distinguished in the discrete drape approach: the mapping schemes, the particle based schemes and the truss based schemes.

Mapping based schemes

Mapping schemes are most commonly employed in commercial packages for drape predictions. A layer of fabric is represented by a square mesh which is fitted onto the drape surface. The mapping scheme is based on the assumption that the fabric only deforms due to shear deformation, and fibre extension can be neglected. The resin, if present, is also neglected during the simulation. The fabric always remains in a fixed position on the draping surface after having been mapped. The shape of the product must be represented in algebraic expressions when modelling draping with a mapping scheme.

Several methods are used to predict the fibre reorientation of the fabric. The geometrical model, also referred to as the kinematics or fishnet model, is a widely used model to predict the resulting fibre reorientation for doubly curved fabric reinforced products. This model was initially described by Mack and Taylor in 1956, based on a pinned-joint description of the weave. The model assumes inextensible fibres pinned together at their crossings, allowing free rotation at these joints. An analytic solution of the fibre redistribution was presented for a fabric oriented in the bias direction on the circumference of simple surfaces of revolution, such as cones, spheres and spheroids. The resulting fibre orientations were solved as a function of the constant height coordinate of the circumference.

From the early 1980s up to the late 1990s many authors presented numerically based drape solutions, based on the same assumptions as Mack and Taylor (see, for example, Robertson *et al.*, 1984; Smiley and Pipes, 1988; Heisey and Haller, 1988; Long and Rudd, 1994; Bergsma, 1995; and Trochu *et*

al., 1996). Typically, these drape models start from an initial point and two initial fibre directions. Further points are then generated at a fixed equal distance from the previous points creating a mesh of quadrilateral cells. There is no unique solution for this geometrical drape method. This problem is generally solved by defining two fibre paths on the drape surface. Bergsma (1995) introduced 'strategies' in order to find solutions for the drape algorithm, without pre-defining fibre paths. Bergsma also included a mechanism to incorporate the locking phenomenon in his drape simulations.

Alternatively to the fishnet model, Van der Weën (1991) presented a computationally efficient energy based mapping method in 1991. Rather than creating a new cell on a geometric basis, the cell in the mesh is mapped onto the drape surface by minimising the elastic energy in the drape cell, while only accounting for the deformation energy used to extend the fibres. Long *et al.* (2002) presented a similar approach based on minimisation of shear strain energy, demonstrating the capability to predict different fibre patterns depending on material type.

The mapping scheme is quite simple in its application and implementation, and requires very limited computational efforts. The results of the mapping scheme agree well with reality if the product shape is convex.

However, the mapping schemes do not predict unique solutions. User interference or 'strategies' are required to solve the drape problem. Inaccurate drape predictions are obtained for products where bridging occurs or when the preform slides over the mould during forming. The scheme is not suited to incorporate the processing conditions accurately during draping or to give an accurate representation of the composite properties. Especially in tight weaves, the error of assuming a zero in-plane fabric shear stiffness during draping leads to errors. From the late 1970s it was shown experimentally that the resin material also affects the deformation properties (Potter, 1979). In addition, the geometrical approach might find infeasible solutions when draping products with holes.

Forming of multi-layered composites is simulated by repeatedly draping single layers of fabric, since the model only represents one layer of fabric. The through-thickness shear interaction between the individual layers is not accounted for.

Particle based schemes

From the first half of the 1990s particle based schemes were used to predict the fabric drape behaviour. The fabric, or cloth, is represented as a discontinuous sheet using micro-mechanical structural elements. These elements, also called particles, interact and must be chosen to be small enough to still represent the weave's behaviour.

An interacting particle model was developed by Breen *et al.* in 1994. Energy functions define the interaction between the particles, placing the particles at the

crossings of the yarns in the fabric. The energy contribution in the particles consists of thread repelling, thread stretching, thread bending, thread trellising and gravity. The total energy in the cloth is simply the sum of the energy of all particles. The modelling strategy for particle based solutions is generally time dependent. In the first time step, the model accounts for the gravity and the collision between the cloth and the drape surface. In the next step a stochastic energy-minimising technique is used to find the local energy minima for the cloth. Finally, permutations are introduced to produce a more asymmetric final configuration.

Similarly to the energy based functions, force based functions were also developed for the interactions of the particles (Colombo *et al.*, 2001). This representation method is applied in commercially available software, since it is computationally more attractive than the energy based particle interaction functions.

Cordier and Magnenat-Thalmann (2002) simulated the cloth behaviour on dressed virtual humans in real time. They proposed a hybrid drape algorithm combining the advantages of physically (particle) based and geometric deformations, avoiding the computationally expensive collision calculations as much as possible. The cloth is segmented into three sections in their simulations. Cloths that remain at constant distance to the drape body are modelled in the first section. Typically, these are stretch cloths. In the second layer, the loose cloth follows predefined discs, representing the limbs. Finally, floating cloth such as skirts is represented in the third section. A force based particle method is used for modelling the floating cloth, incorporating the collision with the underlying body and the cloth itself. Real-time modelling of cloth behaviour is feasible with this approach using middle range computers (up to 1 GHz PCs).

The method requires the mechanical properties of the cloth and the product shape as input. Typically, the method is used for modelling the shape of hanging cloth on objects or humans in the fashion industry. The emphasis is therefore not the deformation and stresses within the fabric but the resulting shape of the cloth as a whole. Possibly, this is why no implementation in the technical industry has been found for this method in the literature.

Truss based schemes

Fabrics are woven using a periodic arrangement of fibre bundles. These periodic arrangements are called Representative Volume Elements (RVE), or unit cells. The fibres in these unit cells can be represented using trusses. The fibre interaction, such as shear-locking of the fabric, is modelled with diagonal stringers. Kato et al. (1999) proposed a unit cell representation based on such a fabric lattice model in 1999.

In 2003, Tanov and Brueggert modelled the inflation of a car side airbag in an FE (Finite Element) simulation, using a loosely woven fabric model. The yarns in the fabric were represented by pinned-joined bars with two locking springs on

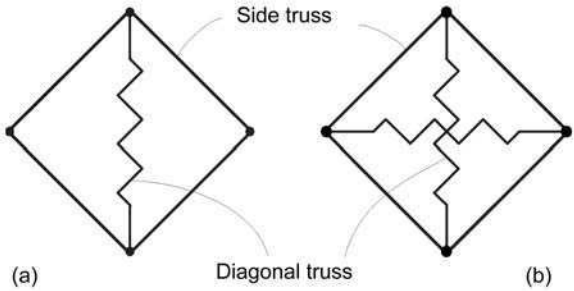

2.1 Schematic representation of the unit cell by truss elements: (a) one diagonal spring element, (b) two diagonal spring elements.

the diagonal of their unit cell. A schematic representation of this unit cell is depicted in Fig. 2.1(b).

Sharma and Sutcliffe (2003) also represented the unit cell in a network of pinned-joined trusses. The edge trusses represent the fibres in the fabric. To introduce shear stiffness in the unit cell, one diagonal spring is introduced, as presented in Fig. 2.1(a). An FE analysis was performed with this pinned-joined net of trusses to predict the draping process.

The advantages of these models are the simple mechanics and ease of use. Little input is required and the simulation time is relatively short compared to continuum based approaches. The resin behaviour is not incorporated in these models. Forming multi-layered composites can be simulated just as with the mapping based schemes since these models are also based on the representation of a single layer of fabric. Through-thickness shear interaction between the fabric layers during forming is not accounted for.

2.2.2 Continuum models

Several constitutive models have been proposed for fabric drape modelling. A distinction can be made between elastic material models, viscous material models and multi-component models. Most of these constitutive models are formulated in a plate or shell theory and implemented in Finite Element formulations.

Elastic models

Finite Element drape simulations by means of elastic models have been applied since the mid 1990s. One of the earliest models was presented by Chen and Govindaraj in 1995. They developed an elastic orthotropic continuum based model to represent the fabric drape behaviour. The material model was based on a flexible shell theory. A non-linear FE formulation was used to predict the forming of a fabric onto a table.

At the same time, Kang and Yu (1995) developed a similar shell based drape model. They used a convective coordinate system in a total Lagrangian formulation with an orthotropic continuum based elastic material model. The nonlinear incremental formulation of the total Lagrangian scheme was solved using Newton's method. Again, the draping of a cloth onto a table was simulated.

A few years later Boisse *et al.* (1997) modelled the bi-axial fabric behaviour in forming processes. The undulation of the yarns in the fabric was accounted for in the bi-axial weave model, assuming fibres with stiffness in the fibre direction only. A refined version of this material model was presented by Boisse *et al.* (2001).

Ivanov and Tabiei (2002) developed an elastic material model based on the RVE of a plain weave fabric. A homogenisation technique accounts for the weave's microstructure, where the yarns are assumed to be transversely isotropic. The shear properties of the fabric are neglected up to the locking angle. On further shear the yarn shear properties are used for the fabric response.

Elastic material laws are fairly simple. The implementation of these models in FE packages is therefore reasonably simple as well, compared to more advanced material models. Generally, the matrix material behaviour is viscoelastic. The properties of the matrix cannot be taken into account accurately with a purely elastic material law. Only single layers of fabric were draped using these models in the literature.

Viscous models

Spencer (2000) modelled the behaviour of impregnated woven fabrics as a viscous fluid. The fibres were assumed inextensible in his model, effectively restraining the deformation of the fluid in the fibre directions. The fluid was also assumed incompressible. In the plane stress situation, the model simplifies to a single parameter model and is able to simulate the draping behaviour of the fabric. Similarly, Spencer (2001) proposed a viscoplasticity model for draping fabric reinforced composites.

The elastic behaviour of the fabric itself is not incorporated in these material models. Therefore, processing-induced fibre stresses are unaccounted for in these models. The models account for the drape behaviour of one layer of fabric only.

Multi-component models

Multi-component models are a combination of several material models. The fibres are often represented as elastic materials in these models. Some models incorporate the fabric shear behaviour, others account for the resin behaviour using viscous material laws.

Sidhu *et al.* (2001) proposed a bi-component FE analysis to model dry fabric forming. The yarns were represented as trusses, using a linear elastic material law. A layer of shell elements accounted for the friction between the yarns and for the locking of the fabric. The material behaviour in the shells was non-linearly elastic and orthotropic. The nodes of the truss and the shell elements were connected in the FE formulation. Friction between the fabric and the tooling was not incorporated in the simulation of the stamping of a spherical shape.

Cherouat and Billoët (2001) presented a model for draping thermoplastic composite materials. The yarns in the fabric were represented using truss elements. The material law representing the yarns was non-linear elastic and based on three deformation mechanics: straightening, relative rotation and tensile stretching. The resin was modelled as an isotropic viscoelastic medium in a layer of shell elements. Again the nodes of the two meshes are connected in the FE simulations. Coulomb friction between the tooling and the fabric was assumed in the forming simulation of a hemispherical product.

McEntee and Ó Brádaigh (1998) modelled the drape behaviour of a multi-layered thermoplastic composite on tools with a single curvature. Two-dimensional elements were stacked through the thickness of the sheet, each ply represented by a row of elements. The constitutive relation in each ply was based on the 'ideal fibre reinforced fluid' model by Rogers (1989). A layer of contact elements was placed between the ply elements. Experiments demonstrated the presence of a resin rich layer between the individual plies during forming, justifying a viscous contact behaviour.

De Luca *et al.* (1998) modelled the drape behaviour of composite laminates in a dynamic explicit FE scheme. Each single fabric layer in the laminate was represented by a layer of elements. Per layer, a bi-phase material model was applied, decoupling the behaviour of the elastic fibres and the viscous matrix. The shell element layers were stacked in the thickness direction of the sheet. Between the shell elements, a 'specialised viscous-friction law' was applied. The model predicts a clear interaction between the laminate lay-up and the drapeability. Experimental results confirm the importance of this interlaminar shear effect. The method provides good results but becomes quite slow by expanding the problem computationally.

Recapitulating, draping can be modelled using the combination of continuum based material models and the FE method. A drape simulation is non-linear due to the large deformations of the fabric during draping and the evolving contact conditions.

The required input consists of the tool and laminate geometry definition, the material property data and the appropriate boundary conditions. The results of the simulation combine the information on the material deformation with the loading required for shaping. The interlaminar shear effects during forming can play a significant role in the drapeability of multi-layered composite com-

ponents. The drape behaviour of multi-layered composites can be modelled by stacking multiple element layers through the thickness of the sheet and connecting them by friction laws.

2.2.3 Multi-layered models

Current drape predictions are based on single fabric layer models or an assembly of single fabric layer models. In some production processes the fabric layers are formed sequentially onto the mould. Interlaminar shear between the individual fabric layers is small in such a production process. Modelling each single fabric layer sequentially suffices for such a process.

However, the interaction between the layers in the sheet is important when draping multi-layered composites. FE simulations with multiple elements through-the-thickness of the sheet are used to account for this interaction between the layers. A friction law accounts for the interlaminar shear between the individual fabric layers. The drawback of using multiple sheet elements on top of each other is the increase of the complexity of the FE model. The total number of degrees of freedom (DOFs) grows linearly with the number of layers in the model and so does the number of contact conditions to be evaluated. A non-linear system of equations has to be solved in the FE representation. The computation times to solve such a non-linear system of equations will easily increase at least quadratically with the increasing number of DOFs. As a result the computation time with increasing layers in the drape simulation behaves correspondingly.

A computationally more efficient method is preferred to predict the drape behaviour of multi-layered fabric composites. This can be achieved in a multi-layer drape material model as presented by Lamers in 2004. This drape model incorporates the inter-ply and intra-ply shear behaviour of multi-layered fabric reinforced composites. The use of multiple elements through-the-thickness of the laminate (and the corresponding contact logic) is avoided by accounting for the interlaminar shear within the multi-layer model. The same type of FE element can be used for the single layer and the multi-layer material model. The number of DOFs in an FE simulation with this multi-layer material model will therefore be equal to the number DOFs of the single layer model. Hence, the computation time for solving the non-linear system of equations will be comparable.

2.3 Continuum based laminate modelling

Continuum mechanics defines the kinematics, stresses, strains and the conservation laws for arbitrary continuous media. Forming simulations require a constitutive relation in addition to these conservation laws.

Here, constitutive relations are presented for single layer and multi-layered composites, based on linear elastic fibres and a Newtonian viscous resin. An

isothermal approach is used in both models, if necessary incorporating an interaction between the warp and fill fibre families. First, a single layer intra-ply material model is presented. This will be extended for multi-layered woven fabric composite material, incorporating inter-ply shear behaviour.

2.3.1 Kinematics

The single layer drape material constitutive equation derived here is an extension to the 'Fabric Reinforced Fluid' (FRF) model by Spencer (2000). Extending the FRF model with elastic components enables the model to incorporate fibre stresses and an elastic fabric shear response in drape predictions. The composite components, the woven fabric and the resin, are subjected to an affine deformation (see Fig. 2.2). The warp and fill fibre families of the fabric are represented by vectors $\boldsymbol{a}$ and $\boldsymbol{b}$; $\varphi(\boldsymbol{X}, t)$ maps the original configuration of a material particle at position $\boldsymbol{X}$ to the current configuration. A continuous distribution of the fibre families is assumed which can vary spatially and in time,

$$\boldsymbol{a}(\boldsymbol{X}, t) = \boldsymbol{F}(\boldsymbol{X}, t) \cdot \boldsymbol{a}_o(\boldsymbol{X}), \qquad \boldsymbol{b}(\boldsymbol{X}, t) = \boldsymbol{F}(\boldsymbol{X}, t) \cdot \boldsymbol{b}_o(\boldsymbol{X}) \tag{2.1}$$

where $\boldsymbol{a}_o(\boldsymbol{X})$, $\boldsymbol{b}_o(\boldsymbol{X})$ are the original fibre orientation unit vectors at $t = 0$ and $\boldsymbol{F}(\boldsymbol{X}, t)$ is the deformation gradient. The length of a fibre may change, leading to a fibre stretch defined as:

$$\lambda_a = \frac{\boldsymbol{a}}{\boldsymbol{a}_o} = \sqrt{\boldsymbol{a}_o \cdot \boldsymbol{F}^T \cdot \boldsymbol{F} \cdot \boldsymbol{a}_o}. \tag{2.2}$$

Allowing fibre extension leads to a change in length of the characteristic vectors $\boldsymbol{a}$ and $\boldsymbol{b}$ of the fibre families. The corresponding unit vectors are introduced as:

$$\boldsymbol{a}^* = \frac{1}{\|\boldsymbol{a}\|}\boldsymbol{a}, \qquad \boldsymbol{b}^* = \frac{1}{\|\boldsymbol{b}\|}\boldsymbol{b}. \tag{2.3}$$

The two bias directions of the weave, $\boldsymbol{s}_1$ and $\boldsymbol{s}_2$, are depicted in Fig. 2.3. The angle ϕ is the angle between the $\boldsymbol{s}_1$ direction and the fibre families a and b,

$$\phi = \frac{1}{2}\arccos(\boldsymbol{a}^* \cdot \boldsymbol{b}^*). \tag{2.4}$$

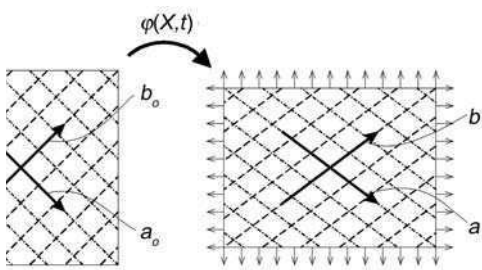

2.2 Affine deformation of fibres and matrix.

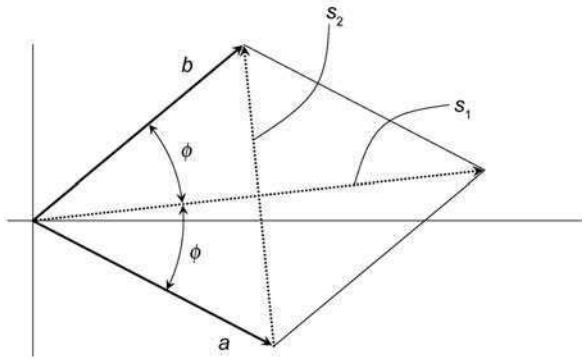

2.3 Directions of the two fibre families a and b and the bias directions s1,2 of the weave.

Often, 2ϕ is referred to as the enclosed fibre angle. The material shear angle θ depends on ϕ as:

$$\theta = 2(\phi_o - \phi), \qquad 2.5$$

where again subscript o refers to the original configuration. Generally, ϕ_o is 45° for woven fabrics.

Constitutive equation for a single layer

The composite material consists of fibres in a textile structure embedded in a matrix, with volume fractions V_f and V_m respectively. The fibre volume is distributed over the fibre families a and b. The sum of the volume fractions evidently equals 1,

$$V_{f_a} + V_{f_b} + V_m = V_f + V_m = 1. \qquad 2.6$$

The matrix will typically have a viscous or viscoelastic response to deformations whereas the fibres have a high tensile stiffness. The fabric structure causes interactions between the fibre families. The amount of fabric shear is restricted and stresses in one fibre direction affect the tensile response in the other direction as well as the shear response. Here, the total Cauchy stress is assumed to be caused by elastic and viscous effects working in parallel,

$$\sigma = \sigma_e + \tau, \qquad 2.7$$

where σ_e is the elastic stress contribution and τ is an extra viscous stress contribution. The elastic and viscous contributions to the stress are solved separately.

The fibres dominate the elastic response. They are modelled as linear elements as a first approximation, having no stiffness properties in any direction but the fibre longitudinal direction. The stress contribution of the fibre is given as:

$$\sigma_a = V_{f_a} E_a (\lambda_a - 1) \boldsymbol{A}^*, \tag{2.8}$$

where $\boldsymbol{A}^*$ is the dyadic product of the unit vector $\boldsymbol{a}^*$,

$$\boldsymbol{A}^* = \boldsymbol{a}^* \boldsymbol{a}^* \tag{2.9}$$

and E_a is the fibre longitudinal modulus.

An analogous relation holds for fibre family b, resulting in:

$$\sigma_b = V_{f_b} E_b (\lambda_b - 1) \boldsymbol{B}^*, \tag{2.10}$$

where

$$\boldsymbol{B}^* = \boldsymbol{b}^* \boldsymbol{b}^* \tag{2.11}$$

and E_b is the longitudinal modulus of fibre family b.

Further elastic effects are found from matrix compression and fabric shear, leading to

$$\sigma_e = \sigma_a + \sigma_b + \sigma_h + \sigma_f, \tag{2.12}$$

where σ_h is the hydrostatic stress and σ_f is the fabric elastic stress. The hydrostatic stress originates from to compression of the matrix:

$$\sigma_h = K \ tr(\epsilon) \boldsymbol{I}, \tag{2.13}$$

where K is the bulk modulus of the matrix, ϵ is the strain tensor and tr is the trace operation.

The fabric elastic stress σ_f is caused by the interaction between the fibres, ultimately leading to shear-locking and wrinkling. This non-linear shear response is modelled as an exponential function of the material shear angle θ as:

$$\sigma_f = V_f m (e^{n\theta} - e^{-n\theta}) \frac{1}{2} (\boldsymbol{C}^* + \boldsymbol{C}^{*T}), \tag{2.14}$$

with

$$\boldsymbol{C}^* = \boldsymbol{a}^* \boldsymbol{b}^*, \tag{2.15}$$

and constants m, n depending on the fabric architecture, which can be evaluated from shear experiments.

The viscous stress contribution is attributed to the matrix, which is described as a linear viscous medium. The stress response of incompressible viscous fluids is represented by an isotropic tensor-valued function of the rate of deformation tensor (Schowalter, 1978). The rate of deformation tensor $\boldsymbol{D}$ is the symmetric part of the velocity gradient,

$$\boldsymbol{D} = \frac{1}{2} \left(\overrightarrow{\nabla} \boldsymbol{v} + \boldsymbol{v} \overleftarrow{\nabla} \right) \tag{2.16}$$

When $\boldsymbol{D}$ meets the incompressibility condition, the most general representation for the viscous stress contribution τ of incompressible viscous fluids can be written as a power series expansion, or:

$$\begin{aligned}\tau &= \tau(\boldsymbol{D}) \\ &= -p\boldsymbol{I} + \psi_1\boldsymbol{D} + \psi_2\boldsymbol{D}^2\end{aligned} \tag{2.17}$$

where p is the hydrostatic pressure, $\boldsymbol{I}$ is the unit tensor and $\psi_{1,2}$ are functions of the invariants $tr\ \boldsymbol{D}^2$ and $tr\ \boldsymbol{D}^3$. In Spencer's FRF model, the viscous stress contribution depends on the rate of deformation and also on the fibre directions:

$$\tau = \tau(\boldsymbol{D}, \boldsymbol{a}^*, \boldsymbol{b}^*). \tag{2.18}$$

Spencer derived an expression for the linear anisotropic viscous response of an incompressible matrix material with inextensible fibres. In this case, the viscous stress contribution is given in its most general form by:

$$\begin{aligned}\tau(\boldsymbol{D}, \boldsymbol{a}^*, \boldsymbol{b}^*) &= 2\eta\boldsymbol{D} + 2\eta_1(\boldsymbol{A}^* \cdot \boldsymbol{D} + \boldsymbol{D} \cdot \boldsymbol{A}^*) + 2\eta_2(\boldsymbol{B}^* \cdot \boldsymbol{D} + \boldsymbol{D} \cdot \boldsymbol{B}^*) + \\ &= 2\eta_3(\boldsymbol{C}^* \cdot \boldsymbol{D} + \boldsymbol{D} \cdot \boldsymbol{C}^{*T}) + 2\eta_4(\boldsymbol{C}^{*T} \cdot \boldsymbol{D} + \boldsymbol{D} \cdot \boldsymbol{C}^*),\end{aligned} \tag{2.19}$$

where η, η_1, η_2, η_3 and η_4 are characteristic anisotropic viscosities generally being functions of the angle between the fibre families a and b. In general, these viscosities will be temperature dependent.

Here, the inextensibility condition is relieved somewhat by assigning a finite stiffness to the fibres. In this way it is not necessary to use Lagrange multipliers in subsequent FE calculations. The fibre stresses are now constitutively determined by the strain in the fibre direction. As a result, $\boldsymbol{D}$ does not necessarily meet the inextensibility conditions in the fibre directions. A modified rate of deformation tensor $\boldsymbol{D}^*$ is introduced to overcome this discrepancy:

$$\boldsymbol{D}^* = \boldsymbol{D} + c_1\boldsymbol{A}^* + c_2\boldsymbol{B}^* + c_3\boldsymbol{I} \tag{2.20}$$

where $\boldsymbol{D}^*$ is the deviatoric part, satisfying the inextensibility and incompressibility conditions:

$$\begin{aligned}\boldsymbol{A}^* : \boldsymbol{D}^* &= 0, \\ \boldsymbol{B}^* : \boldsymbol{D}^* &= 0, \\ \boldsymbol{I} : \boldsymbol{D}^* &= 0.\end{aligned} \tag{2.21}$$

With these conditions it can be found that the unknowns $c_{1,2,3}$ are:

$$\begin{aligned}c_1 &= \frac{1}{d}\left[(3g_B - \mathrm{I}_B^2)\boldsymbol{A}^* : \boldsymbol{D} - (3g_{AB} - \mathrm{I}_A\mathrm{I}_B)\boldsymbol{B}^* : \boldsymbol{D} + (g_{AB}\mathrm{I}_B - \mathrm{I}_A g_B)\mathrm{I}_D\right] \\ c_2 &= \frac{1}{d}\left[(3g_A - \mathrm{I}_A^2)\boldsymbol{B}^* : \boldsymbol{D} - (3g_{AB} - \mathrm{I}_A\mathrm{I}_B)\boldsymbol{A}^* : \boldsymbol{D} + (g_{AB}\mathrm{I}_A - g_A\mathrm{I}_B)\mathrm{I}_D\right] \\ c_3 &= \frac{1}{d}\left[(g_{AB}\mathrm{I}_B - \mathrm{I}_A g_B)\boldsymbol{A}^* : \boldsymbol{D} + (g_{AB}\mathrm{I}_A - g_A\mathrm{I}_B)\boldsymbol{B}^* : \boldsymbol{D} - (g_{AB}^2 - g_A g_B)\mathrm{I}_D\right]\end{aligned} \tag{2.22}$$

where

$$\begin{aligned}d &= g_A\mathrm{I}_b^2 + 3g_{AB}^2 - 2g_{AB}\mathrm{I}_A\mathrm{I}_B + g_B\mathrm{I}_A^2 - 3g_A g_B, \\ \mathrm{I}_A &= tr\ \boldsymbol{A}^*, \quad \mathrm{I}_B = tr\ \boldsymbol{B}^*, \quad \mathrm{I}_D = tr\boldsymbol{D}\end{aligned}$$

and

$$g_A = \boldsymbol{A}^* : \boldsymbol{A}^*, \quad g_B = \boldsymbol{B}^* : \boldsymbol{B}^*, \quad g_{AB} = \boldsymbol{A}^* : \boldsymbol{B}^*.$$

The total stress in (2.7) is found by using (2.20) in (2.19) and combining the terms in equations (2.8, 2.10, 2.12, 2.14, 2.19) to:

$$\begin{aligned}\sigma = &-p\boldsymbol{I} + V_{f_a}E_a(\lambda_a - 1)\boldsymbol{A}^* + V_{f_b}E_b(\lambda_b - 1)\boldsymbol{B}^* + \\ &+ \frac{1}{2}V_f m(e^{n\theta} - e^{-n\theta})\left(\boldsymbol{C}^* + \boldsymbol{C}^{*T}\right) + \\ &+ V_m[2\eta\boldsymbol{D}^* + 2\eta_1(\boldsymbol{A}^* \cdot \boldsymbol{D}^* + \boldsymbol{D}^* \cdot \boldsymbol{A}^*) + 2\eta_2(\boldsymbol{B}^* \cdot \boldsymbol{D}^* + \boldsymbol{D}^* \cdot \boldsymbol{B}^*) + \\ &+ 2\eta_3\left(\boldsymbol{C}^* \cdot \boldsymbol{D}^* + \boldsymbol{D}^* \cdot \boldsymbol{C}^{*T}\right) + 2\eta_4\left(\boldsymbol{C}^{*T} \cdot \boldsymbol{D}^* + \boldsymbol{D}^* \cdot \boldsymbol{C}^*\right)], \end{aligned} \tag{2.23}$$

The constitutive relation is symmetric with respect to the fibre families a and b when the fibre families are mechanically equivalent. This symmetry in the constitutive relation reduces the number of independent parameters in the extra viscous stress contribution as $\eta_1 = \eta_2$ and $\eta_3 = \eta_4$ (Spencer, 2000). Three parameters η, η_1 and η_3, generally being functions of cos 2ϕ, are required to determine the extra viscous stress response of the fabric. They can either be even or odd functions of cos 2ϕ.

2.4 Multilayer effects

A composite laminate consists of multiple layers, generally with different fibre orientations. A multilayer model must allow these individual plies to slide with respect to each other and deform individually. Figure 2.4 illustrates the deformation of a three ply laminate due to a load on the centre ply. The laminate deforms from its original configuration to a current configuration. The layers are stacked on each other in the original configuration, having independent fibre orientations $\boldsymbol{a}_i$ and $\boldsymbol{b}_i$, where i is the ply index. The plies are allowed to deform individually, conforming to their fibre orientations. The strains ϵ_i, rotation ω_i, the velocities $\boldsymbol{v}_i$ and the rates of deformation $\boldsymbol{D}_i$ will generally also be non-uniform over the laminate thickness as a result.

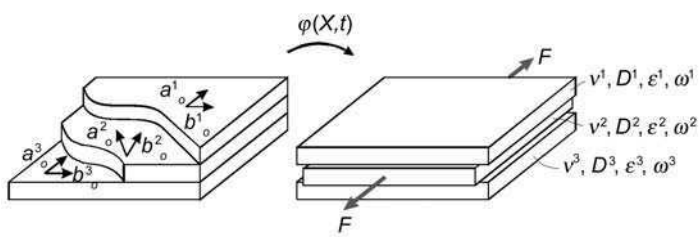

2.4 Deformation of the individual layers during composite forming.

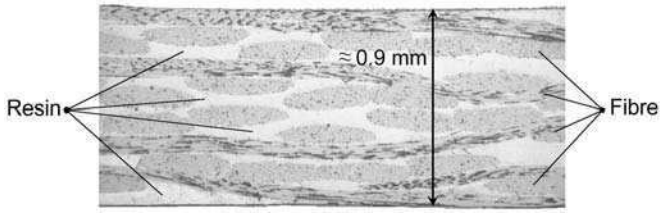

2.5 Cross-sectional view of an 8H satin glass fibre weave reinforced PPS, illustrating the resin rich layers between the fabric plies.

Since the individual plies in the laminate can have different velocities, the interface between these plies must deform correspondingly. Therefore, a slip law needs to be defined which is able to describe the sliding of the individual plies.

Figure 2.5 shows a microscopic view of the cross-section of a compression moulded glass poly(phenylene sulphide) (PPS) laminate, reinforced with four layers of 8H satin fabric. The horizontal glass fibre yarns in dark grey indicate the separate fabric layers. Some yarn contact is noticed in Fig. 2.5. However, resin is observed between most of the plies. These plies are separated by the lighter coloured thin PPS layers. Based on the observations of these resin rich layers between the plies and following the work of McEntee and Ó Brádaigh (1998), the interlaminar behaviour is assumed to be viscous. This leads to a viscous slip law expressed in the velocity differences between adjacent plies,

$$\boldsymbol{v}^{j}_{rel} = \boldsymbol{v}^{i+1} - \boldsymbol{v}^{i}, \qquad 2.24$$

where the suffix i indicates the ply and j indicates the interface layer between the plies i and $i+1$. When assuming a friction law which depends linearly on the velocity difference between the plies, the interface traction γ^j is defined as:

$$\gamma^j = \frac{1}{\beta_j}\boldsymbol{v}^{j}_{rel}, \qquad 2.25$$

with a slip factor β_j. This constant friction factor is derived as

$$\beta_j = \frac{h_j}{\eta_j}, \qquad 2.26$$

where h_j is the averaged thickness of the interface layer and η_j the viscosity of the interface layer.

2.5 Parameter characterisation

The material property data need to be determined before the constitutive relations (2.23) and (2.25) can be employed in composite forming simulations. Both the intra-ply and inter-ply composite properties need to be characterised. Materials characterisation is discussed in Chapter 1.

There is little standardisation in the experimental characterisation of pre-impregnated technical fabrics at production temperature. Some standardisation for measuring the intra-ply response of dry textiles is available in the garment industry. The Kawabata Evaluation System for Fabrics (KES-F) (Kawabata, 1975) is used to measure the formability of fashion cloths at room temperature. Unfortunately, KES-F is not applicable for testing pre-impregnated composite materials since it is not designed to test at high temperatures, to apply large shear deformations or to measure at relatively high loads. The topic of standardisation is discussed further in Chapter 13.

The number of intra-ply material parameters required for the single layer material model is quite extensive. The fibre properties are usually available in the literature (e.g., Peters, 1998). The other material properties, m, n, η, η_1, η_2, η_3 and η_4, need to be quantified experimentally. Picture frame experiments can be used to determine these intra-ply properties. The inter-ply composite properties can be determined using pull-out tests (Murtagh and Mallon, 1997).

2.5.1 Picture frame

McGuinness and Ó Brádaigh (1997) presented the picture or trellis frame experiment in 1997 in order to measure the in-plane response of woven fabric reinforced composites. Since then, several authors (Prodromou and Chen, 1997; Mohammed *et al.*, 2000; Peng *et al.*, 2002) applied the picture frame experiment to determine the properties of dry and pre-impregnated fabrics. An initially square frame deforms into a rhombus, imposing a shear deformation onto the fabric. The fabric is placed in the frame with the fibre directions parallel to the arms of the frame, as shown in Fig. 2.6. In this manner the fabric deforms without extension in the fibre directions. Left or right shear deformations, denoted with the subscripts l and r, are imposed on the fabric by extending the frame in the vertical or horizontal direction respectively. The shear response of the composite can be determined by measuring the load response $F_{l,r}$ of the frame. The load,

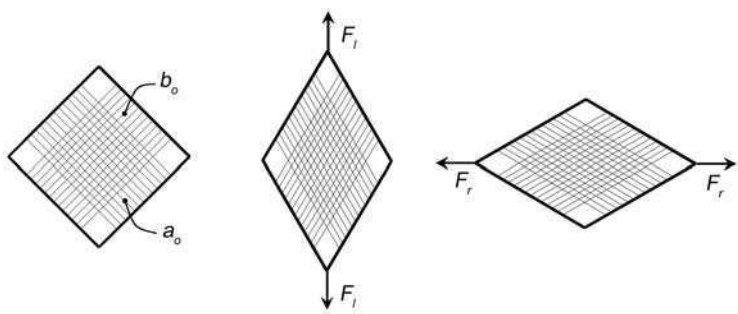

2.6 Schematic deformation of the composite in the picture frame experiment; from left to right: initial configuration, left shear and right shear.

required to deform the fabric, is measured as a function of the crosshead displacement in a tensile testing machine. The shear response of the weave can be unsymmetric, when it different for left and right shear (McGuinness and Ó Brádaigh, 1997). Impregnated composites are tested above the glass transition or melt temperature of the matrix material. The entire picture frame, including the specimen, is placed in an oven in order to perform these high-temperature tests. Ideally, the temperature dependent viscosities are determined for a range of temperatures, appropriate for the composite forming conditions.

Picture frame kinematics

The crosshead displacement of the tensile testing machine causes the frame to shear. The velocity at which the crosshead travels is usually constant during the test, resulting in a variation of the shear rate of the fabric. The fabric deformation can be expressed in terms of the crosshead displacement and velocity.

A schematic view of the frame in the undeformed and deformed state is shown in Fig. 2.7, using the bias directions as the *xy*-coordinate system. The frame with side length l_f and initial frame angle ϕ_o is shown on the left-hand side, using one line of symmetry. The deformed frame (after right shear) is presented on the right-hand side, where also the displacement Δu_r and its velocity v_r for right shear are indicated. The length l_r of the frame in the deformed state is given as a function of the displacement by:

$$l_r = l_f \cos \phi_o + \Delta u_r. \qquad 2.27$$

Hence the frame angle ϕ can be expressed in terms of the displacement Δu_r and the length of the sides of the picture frame l_f,

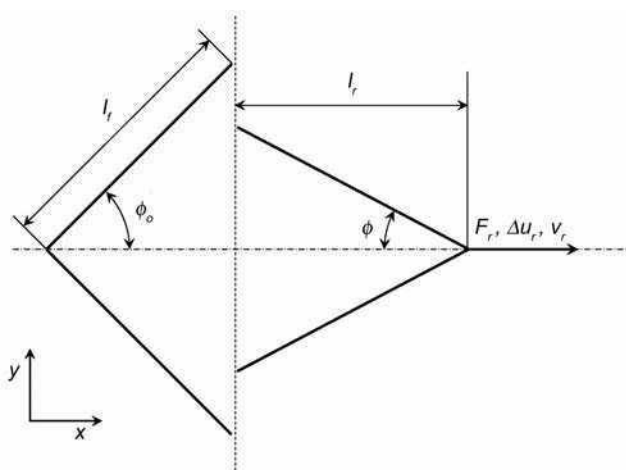

2.7 Schematic view on half of the picture frame: undeformed (left) and deformed shape (right).

$$\phi = \arccos\left(\cos\ \phi_o + \frac{\Delta u_r}{l_f}\right). \tag{2.28}$$

When a left shear deformation is applied, the crosshead displacement Δu_l results in a frame angle ϕ given by:

$$\phi = \arcsin\left(\sin\ \phi_o + \frac{\Delta u_l}{l_f}\right), \tag{2.29}$$

where Δu_l is in the positive vertical direction. The material shear angle θ can be found straightforwardly by substituting equation (2.28) or (2.29) into equation (2.5).

The fibre directions during testing are parallel to the sides of the frame,

$$\boldsymbol{a} = (\cos\phi, -\sin\phi, 0), \quad \boldsymbol{b} = (\cos\phi, \sin\phi, 0). \tag{2.30}$$

The rate of change of the frame angle for right shear deformation can be expressed in terms of the velocity:

$$\dot{\phi} = -\frac{v_r}{l_f \sin\phi}, \tag{2.31}$$

and the time derivative of the frame angle for left shear deformation is:

$$\dot{\phi} = \frac{v_l}{l_f \cos\phi}. \tag{2.32}$$

Finally, the rate of deformation tensor $\boldsymbol{D}$ is (Spencer, 2000):

$$\boldsymbol{D} = \begin{bmatrix} -\tan\phi & 0 & 0 \\ 0 & \cot\phi & 0 \\ 0 & 0 & -2\cot\phi \end{bmatrix} \dot{\phi}, \tag{2.33}$$

where the out-of-plane component follows from the assumption of incompressibility.

Considering that the fabric is in a state of plane stress without fibre elongation, the stress components can be found from equation (2.23):

$$\begin{aligned}
\sigma_{xx} &= \tfrac{1}{2} V_f m\left(e^{n\theta} - e^{-n\theta}\right) a_x b_x + \\
&\quad + 2V_m D_{xx}\left(\eta + 2\eta_1 {a_x}^2 + 2\eta_s {b_x}^2 + 2(\eta_3 + \eta_4) a_x b_x\right) - 2V_m \eta D_{zz} \\
\sigma_{xy} &= \tfrac{1}{4} V_f mleft(3^{n\theta} - e^{-n\theta})\left(a_x b_y + a_y b_x\right) + \\
&\quad + 2V_m D_{xx}\left(\eta_1 a_x a_y + \eta_2 b_x b_y + \eta_3 a_y b_x + \eta_4 a_x b_y\right) + \\
&\quad + 2V_m D_{yy}\left(\eta_1 a_x a_y + \eta_2 b_x b_y + \eta_3 a_x b_y + \eta_4 a_y b_x\right) \\
\sigma_{yy} &= \tfrac{1}{2} V_f m\left(e^{n\theta} - e^{-n\theta}\right) a_y b_x + \\
&\quad + 2V_m D_{yy}\left(\eta + 2\eta_1 {a_y}^2 + 2\eta_2 {b_y}^2 + 2(\eta_3 + \eta_4) a_y b_y\right) - 2V_m \eta D_{zz}
\end{aligned} \tag{2.34}$$

where all fabric deformation characteristics are defined in (2.5, 2.30 and 2.33).

Picture frame equilibrium

The shear fixture imposes a shear deformation on the fabric. When neglecting inertia effects, the stress and the strain distributions in the specimen are homogeneous as a result. The external loading as imposed by the tensile testing machine must be in equilibrium with these stresses, multiplied by the appropriate cross-sectional area. Volume changes can be assumed negligible during testing (McGuinness and Ó Brádaigh, 1997). The thickness of the composite thus increases during testing, inversely related to the reduction in surface area of the specimen. The thickness h during testing can be expressed in terms of the frame angle ϕ as:

$$h = \frac{h_o}{\sin 2\phi}, \tag{2.35}$$

where h_o is the initial thickness of the specimen.

Performing a static analysis (Lamers, 2004) provides the load response of the frame corresponding to a homogeneous fabric stress distribution. Analysing right shear deformation leads to:

$$F_r = \frac{h_o}{\sin 2\phi}(\sigma_{xx} l_f \sin\phi - \sigma_{yy} l_f \cot\phi \cos\phi) \tag{2.36}$$

and for left shear the load response is found as:

$$F_l = \frac{h_o}{\sin 2\phi}(\sigma_{xx} l_f \tan\phi \sin\phi - \sigma_{yy} l_f \cos\phi) \tag{2.37}$$

The load response of the fabric is found in terms of the material parameters by substituting (2.34) into (2.36) and (2.37). A non-linear fitting procedure is required to fit the material parameters m, n, η, η_1, η_2, η_3 and η_4 on the experimental data.

Picture frame experiments

Picture frame tests were performed on pre-consolidated laminates. Four layered glass fibre reinforced PPS 8H satin weave (Ten Cate CetexSS303) laminates were pressed. The PPS has a melting temperature of 285ºC. The specimens were prepared to fit into the frame. The dimensions of the specimens are shown in Fig. 2.8. Some fibres were removed in the zone next to the central area which delays inhomogeneous deformation due to wrinkling. Five experiments were performed at 300ºC and three at 350ºC for right shear deformation. Also, two tests were performed for left shear deformation at 300ºC. The velocity of the traverse of the tensile testing rig was set at 1000 mm/min for all

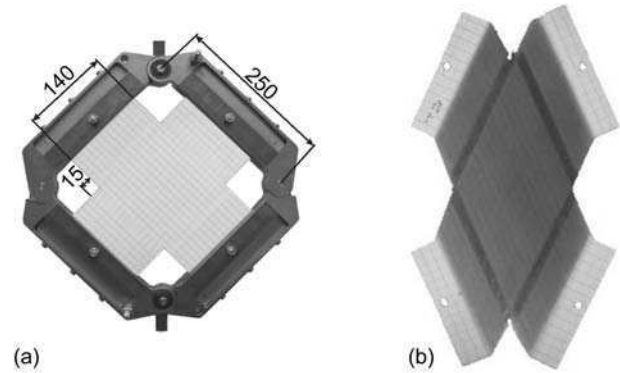

2.8 (a) Composite clamped in the picture frame prior to testing. (b): Deformed shape of the specimen after the shear test. All dimensions are in mm.

tests. The deformed shape of the specimens is depicted in Fig. 2.8b. The corresponding load versus material deformation angle response of the tests is given in Fig. 2.9. This load versus angle response is typical for the picture frame tests. The load increases with increasing deformation angle in a non-linear manner. The load response of the specimens tested at 350ºC is significantly lower than the load response for the specimens tested at 300ºC. The lower load can be attributed to the lower viscosity of the PPS matrix material at higher temperatures, resulting in a lower shear resistance of the viscous part of the composite. The load versus angle response of the impregnated fabric was independent of the shearing direction. The composite intra-ply shear behaviour is symmetrical.

In-plane symmetrical behaviour implies that the composite viscosities are mutually related (Spencer, 2000). The viscosities η_1 and η_2 are equal even functions of cos 2ϕ, while η_3 and η_4 are equal odd functions of cos 2ϕ. Fitting

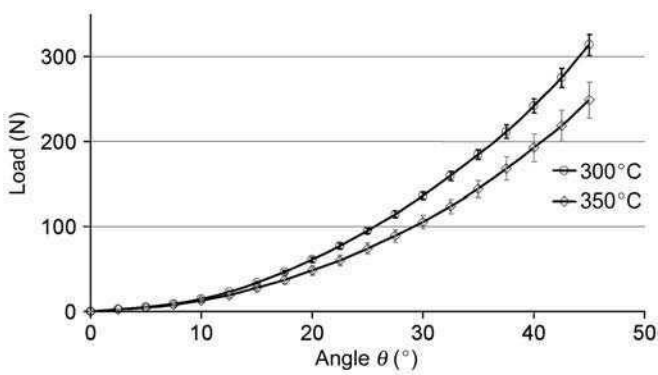

2.9 Load versus material deformation angle response during the picture frame test; test velocity 1000 mm/min, temperatures 300ºC and 350ºC.

Table 2.1 Fitted intra-ply material data for 8H glass PPS (Cetex SS303)

Property		$2\phi \leq \frac{1}{2}\pi$	$2\phi > \frac{1}{2}\pi$	$2\phi \leq \frac{1}{2}\pi$	$2\phi > \frac{1}{2}\pi$
m	MPa	0.218	0.218	0.182	0.182
n	–	3.290	3.290	3.156	3.156
η	MPa s	0.281	0.281	0.205	0.205
η_1	Pa s	16.503	16.503	30.315	30.315
η_2	Pa s	16.503	16.503	30.315	30.315
η_3	MPa s	−0.394	0.394	−0.335	0.335
η_4	MPa s	−0.394	0.394	−0.335	0.335

the material property data on the experimental results gives the parameter values listed in Table 2.1.

2.5.2 Bias extension

Alternatively, the intralaminar shear response of the composite can be characterised with a bias extension experiment. A strip of the composite reinforced with a ±45° woven fabric is extended in the bias direction as illustrated in Fig. 2.10. Three zones can be distinguished in the deformed specimen. The central area (*I*) shears uniformly, with an enclosed angle 2ϕ. Neglecting fibre extension, this angle is related to the clamp displacement Δu by

$$\phi = \arccos\left(\frac{1}{\sqrt{2}} \cdot \left(1 + \frac{\Delta u}{L_o - w_o}\right)\right), \qquad 2.38$$

with L_o and w_o as the original length and width of the sample respectively. The clamps induce an area with zero shear (*III*), whereas the intermediate zone (*II*) has a material shear angle θ_{II} which is half of the value in the central zone,

$$\theta_{II} = \tfrac{1}{2}\theta = \phi_o - \phi, \qquad 2.39$$

with ϕ_o as the half original enclosed angle (45°).

The stress state is uniaxial in the central region, with

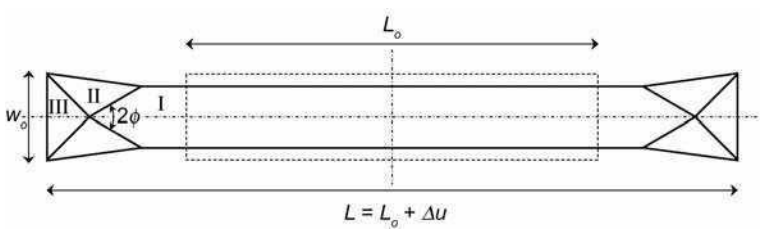

2.10 Schematic view of the bias extension specimen. The undeformed geometry is indicated with dashed lines.

$$\sigma_{xx} = \frac{F}{wh} = \frac{F\cos\phi}{w_o h_o \sqrt{2}}, \qquad 2.40$$

where F is the external force.

Combining equations (2.38), (2.40) with the relations (2.30–2.33) presented earlier for the picture frame analysis and the constitutive equation (2.23) leads to a nonlinear equation which can be fitted to the experimental force-displacement results. Note, however, that these data are obtained for non-zero fibre stresses, contrary to the picture frame results. This biaxial stress state is likely to affect the shear response of the fabric reinforced composite. This phenomenon is beyond the scope of the current chapter.

2.5.3 Pull-out

The individual plies slide with respect to each other during draping. This interlaminar behaviour is accounted for in the multi-layer material model. A viscous traction was assumed to model this phenomenon. This traction can be measured using fabric pull-out tests. Four layers of fabric are placed in a tensile testing machine in a temperature controlled environment (Murtagh and Mallon, 1997). The middle layers are then pulled out of the other two (see Fig. 2.11), while measuring the load as a function of the crosshead velocity. After a certain time, the average surface traction (the shear load divided over the current contact area) will attain a constant value. The average interlaminar slip factor β can be determined by elaborating (2.25) to

$$\beta = \frac{v_{rel}}{\gamma} = \frac{2wL(t)V}{F(t)}, \qquad 2.41$$

with V as the crosshead velocity, F as the tensile load, w as the width of the specimen and L as the momentary contact length.

Alternatively, a resin rich layer can be assumed of a certain thickness as found from microscopy (Fig. 2.5), similarly to McEntee and Ó Brádaigh (1998). The slip factor can be determined from (2.26), using this interface layer thickness and the resin viscosity data.

The actual tribology of these composite systems is complicated, however. The response is time dependent while the steady state values vary with fibre

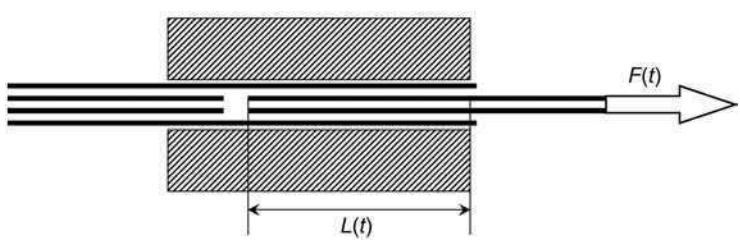

2.11 Schematic view of the pull-out experiment on a four layered laminate.

orientation, pressure, temperature and velocity. The simple viscous law introduced here is only a first approximation which should be adapted according to further findings.

Similar arguments hold for the friction between the composite and the tools, which can have a major effect on the draping process. The same pull-out set-up can be used to characterise ply-tool friction. The tools are placed on both sides of the composite and pressed with a pre-set load on the composite surface. The full laminate is now pulled through or out of the tooling blocks. The load displacement data can now be translated to a ply-tool slip factor or friction coefficient.

2.6 Future trends

Realistic process simulations of the composite forming process are within reach for product development purposes. Simulations can be made with acceptable computational efforts. The presented constitutive relations provide a basic framework which captures the most important phenomena: intra-ply shear of a fabric reinforced fluid, elastic fibres, shear locking of the fabric and inter-ply shear in multi-layered composite laminates. The required material property data can be determined by conceptually simple experiments in combination with nonlinear regression.

The various elements can be elaborated further, as the computer performance is still increasing rapidly and further complexities can be introduced. The description of interaction between the yarns in the fabric needs to be improved. Biaxial stresses have been shown to have a distinct effect on the fabric response (Boisse *et al.*, 2001). This, however, also holds for intralaminar shear, where little experimental data are available at present. The constitutive equations need to be established and appropriate characterisation methods need to be developed.

This argument holds even more for the interlaminar shear and the friction of the laminate with the forming tools. It is evident that the governing parameters are pressure, temperature, velocity, time, fabric structure and fibre orientation. However, the exact physics are poorly understood to date. The underlying mechanisms need to be identified, modelled and quantified in order include a more accurate description in the forming simulations.

Accurate process simulations further require the material property data over the full temperature range in the process. This implies a huge experimental effort, considering the vast number of combinations of fibres, matrices and fabric architectures. Micromechanical models can be used as an alternative to predict the composite properties with only the constituent properties and the reinforcement structure as an input. It will be very difficult to keep the characterisation efforts within reasonable limits without this type of model.

Finally, the success of forming simulations depends strongly on the ability of designers to work with them. On one hand, the developers need to make their software user friendly to make it accessible to the designer. On the other hand,

the composite designer has to be aware of the complex material behaviour and the resulting effects on the forming process. This can only be achieved with thorough education and experience. Using these simulations as a black box is an approach which is doomed to fail.

2.7 References

Bergsma O, *Three-dimensional Simulation of Fabric Draping*, PhD thesis Delft University of Technology, 1995.

Boisse P, Borr M, Buet K and Cheroaut, A, 'Finite element simulation of textile composite forming including the biaxial fabric behaviour', *Composites Part B*, 1997, **28**, 453–464.

Boisse P, Gasser A and Hivet G, 'Analyses of fabric tensile behaviour: determination of the biaxial tension-strain surface and their use in forming simulations', *Composites Part A*, 2001, **32**, 1395–1414.

Breen DE, House DH and Wozny MJ, 'A particle-based model for simulating the draping behavior of woven cloth', *Textile Research Journal*, 1994, **64**, 663–685.

Chen B, and Govindaraj M, 'A physically based model of fabric drape using flexible shell theory', *Textile Research Journal*, 1995, **65**, 324–330.

Cherouat A and Billoët JL, 'Mechanical and numerical modelling of composite manufacturing processes in deep-drawing and laying-up of thin pre-impregnated woven fabrics', *Materials Processing Technology*, 2001, **118**, 460–471.

Colombo G, Prati M and Rizzi C, 'Design and evaluation of a car soft top' In *XII ADM International Conference*, Rimini, Italy, 2001.

Cordier F and Magnenat-Thalmann N, 'Real-time animation of dressed virtual humans' *Computer Graphics Forum (Eurographics 2002)*, **21**, 327–336.

De Luca P, Lefébure P and Pickett AK, 'Numerical and experimental investigation of some press forming parameters of two fibre reinforced thermoplastics: APC2-AS4 and PEI-CETEX', *Composites Part A*, 1998, **29**, 101–110.

Heisey FL and Haller KD, 'Fitting woven fabric to surfaces in three dimensions', *Journal of the Textile Institute*, 1988, **2**, 250–263.

Ivanov I and Tabiei A, 'Flexible woven fabric micromechanical material model with fiber reorientation', *Mechanics of Advanced Materials and Structures*, 2002, **9**, 37–51.

Kang TJ and Yu WR, 'Drape simulation of woven fabric by using the finite- element method', *Journal of the Textile Institute*, 1995, **86**, 635–648.

Kato S, Yoshino T and Minami, H, 'Formulation of constitutive equations for fabric membranes based on the concept of fabric lattice model', *Engineering Structures*, 1999, **21**, 691–708.

Kawabata S, *The standardization and analysis of hand evaluation*, Osaka, Japan, Hand evaluation and standardization committee of the Textile Machinery Society of Japan, 1975.

Lamers EAD, *Shape distortions in fabric reinforced composite products due to processing induced fibre reorientation*, PhD thesis University of Twente, 2004.

Lim T-C and Ramakrishna S, 'Modelling of composite sheet forming: a review', *Composites Part A*, 2002, **33**, 515–537.

Long AC and Rudd CD 'A simulation of reinforcement deformation during the production of preforms for liquid moulding processes', *Journal of Engineering Manufacture*, 1994, **208**, 269–278.

Long AC, Souter B, Robitaille F and Rudd CD, 'Effects of fibre architecture on reinforcement deformation', *Plastics Rubber and Composites*, 2002, **31**, 87–97.

Mack C and Taylor H, 'The fitting of woven cloth to surfaces', *Journal of Textile Institute*, 1956, **47**, 477–487.

McEntee SP and Ó Brádaigh CM, 'Large deformation finite element modelling of single-curvature composite sheet forming with tool contact', *Composites Part A*, 1998, **29**, 207–213.

McGuinness GB and Ó Brádaigh CM, 'Development of rheological models for forming flows and picture-frame shear testing of fabric reinforced thermoplastic sheets', *Journal of Non-Newtonian Fluid Mechanics*, 1997, **73**, 1–28.

Mohammed M, Lekakou C, Dong L and Bader MG, 'Shear deformation and micromechanics of woven fabrics', *Composites Part A*, 2000, **31**, 299–308.

Murtagh A and Mallon P. 'Characterisation of shearing and frictional behaviour during sheet forming', In Bhattacharyya D and Pipes R, *Composite sheet forming*, Composite material series vol. 11, Amsterdam, Elsevier, 1997, 163–214.

Peng XQ, Xue P, Cao J, Lussier DS and Chen J, 'Normalization in the picture frame test of woven composites, length or area', In *Proceedings of the 5th ESAForm conference on material forming*, Krakow, Poland, 2002, Akapit Publishers.

Peters ST, *Handbook of composites*, London, Chapman & Hall, 1998.

Potter KD, 'The influence of accurate stretch data for reinforcements on the production of complex structural mouldings', *Composites*, 1979, **10**, 161–167.

Prodromou AG and Chen J, 'On the relationship between shear angle and wrinkling of textile composite preforms', *Composites Part A*, 1997, **28A**, 491–503.

Robertson RE, Hsiue ES and Yeh GSY, 'Fibre rearrangements during the moulding of continuous fibre composites II', *Polymer Composites*, 1984, **5**, 191–197.

Rogers TG, 'Rheological characterisation of anisotropic materials', *Composites*, 1989, **20**, 21–27.

Schowalter WR, *Mechanics of non-Newtonian fluids,* Oxford, Pergamon Press, 1978.

Sharma SB and Sutcliffe MPF, 'A simplified finite element approach to draping of woven fabric', In *Proceedings of the 6th ESAFORM conference on material forming*, Salerno, Italy, 2003, Nuova Ipsa Editore.

Sidhu RMJS, Averill RC, Riaz M and Pourboghrat F, 'Finite element analysis of textile composite preform stamping', *Composite Structures*, 2001, **52**, 483–497.

Smiley AJ and Pipes RB, 'Analysis of the diaphragm forming of continuous fiber reinforced thermoplastics', *Journal of Thermoplastic Composite Materials*, 1988, **1**, 298–321.

Spencer AJM, 'Theory of fabric-reinforced viscous fluids', *Composites Part A*, 2000, **31**, 1311–1321.

Spencer AJM, 'A theory of viscoplasticity for fabric-reinforced composites', *Journal of the Mechanics and Physics of Solids*, 2001, **49**, 2667–2687.

Tanov RR and Brueggert M, 'Finite element modelling of non-orthogonal loosely woven fabrics in advanced occupant restraint systems', *Finite Elements in Analysis and Design*, 2003, **39**, 357–367.

Trochu F, Hammami A and Benoit Y, 'Prediction of fibre orientation and net shape definition of complex composite parts', *Composites Part A*, 1996, **27**, 319–328.

Weën F van der, 'Algorithms for draping fabric on doubly-curved surfaces', *International journal for numerical methods in engineering*, 1991, **31**, 1415–1426.